

MEASURING FOREST CANOPY WATER MASS IN THREE DIMENSIONS USING TERRESTRIAL LASER SCANNING

A. Elsherif^{1*}, R. Gaulton², J. P. Mills³, E. Sharaf El Din¹

¹ Faculty of Engineering, Tanta University, Tanta, Egypt – ahmed.elsherif@f-eng.tanta.edu.eg

² School of Natural and Environmental Sciences, Newcastle University, Newcastle upon Tyne, UK - rachel.gaulton@newcastle.ac.uk

³ School of Engineering, Newcastle University, Newcastle upon Tyne, UK – jon.mills@newcastle.ac.uk

¹ Faculty of Engineering, Tanta University, Tanta, Egypt – essam.helmy@f-eng.tanta.edu.eg

KEY WORDS: Climate Change, LiDAR, Plant Water Content, Tree Stress, Forest Health.

ABSTRACT:

Canopy water mass is an important plant characteristic that can indicate the water status of vegetation. However, the parameter remains under-investigated because measuring it requires defoliating the canopy. This study introduced a non-destructive approach to estimate canopy water mass using terrestrial laser scanning data. Tree 3D models were generated from dual-wavelength TLS data for six forest canopies, then the models were utilized in estimating the canopy LAI, total leaf area, and vertical profiles of canopy leaf area. The estimates were then coupled with canopy equivalent water thickness estimates and vertical profiles of canopy water mass were generated. The results revealed some over- and underestimation in the estimated LAI, but the obtained accuracy was considered sufficient as leaf-on point clouds were used to generate the 3D models. The vertical profiles of canopy water mass showed that the leaf area distribution within the canopy, and the canopy architecture were the main parameters affecting the water mass distribution within the canopy, with mid canopy layers having higher water mass than the other canopy layers. This study showed the potential of TLS to estimate canopy water mass, but controlled experiments that include defoliating canopies are still needed for a direct and accurate validation of the TLS estimates of canopy water mass.

1. INTRODUCTION

Forests play a crucial role in sustaining life on Earth, serving as a carbon sink and regulating the water cycle (Mengist et al., 2019). Furthermore, forests protect soil from erosion, resist landslides and floods, shelter more than 80% of terrestrial biodiversity, and provide humanity with food, fuel, timber, and other goods (Aerts et al., 2011). Climate change has severe impacts on forests, including the increase in rate and intensity of wildfires, the reduction of tree growth and productivity due to warmer temperatures and more frequent and intense droughts, the spread of pathogens and pests, and the rise of tree mortality rate (Keenan, 2015; Sturrock et al., 2011). Such impacts are expected to worsen over the next decades, as climate change is projected to intensify (Masson-Delmotte et al., 2021), which makes continuous monitoring of forest health essential. For this, determining forest canopy water status has been a widely adopted approach.

Various measurements can reflect the water status of vegetation, including the leaf water potential, the leaf Relative Water Content (RWC, %), and the leaf Equivalent Water Thickness (EWT, g cm⁻²). Leaf water potential is measured using a pressure chamber (Scholander et al., 1964), and is considered an accurate indicator of vegetation hydration level (Boyer, 1967; Cochard et al., 2001; Rodriguez-Dominguez et al., 2022). Leaf RWC, given as the leaf water content divided by its water content when it is fully saturated with water, reflects the balance between water in leaf tissue and its transpiration rate (Zhang et al., 2012). A drop in leaf RWC corresponds to water deficit stress, rendering it a robust indicator of plant water status (Ali et al., 2022; Kettani et al., 2023; Yamasaki et al., 1999). Leaf EWT is the amount of water per unit leaf area, and like RWC, a

reduction in EWT indicates a water-stressed plant (Féret et al., 2019; Tucker et al., 1980).

Nevertheless, obtaining the aforementioned measurements on a large scale (canopy and plot levels) is labour intensive, costly, and time consuming, as it involves destructive sampling, weighing, and drying large amounts of leaves from multiple canopy layers (Yilmaz et al., 2008). Thus, numerous studies have used remote sensing data in form of vegetation indices to retrieve RWC and EWT in a rapid, non-destructive manner (Gao et al., 1995; Kothari et al., 2023; Meiyani et al., 2022; Seelig et al., 2008). However, applying such indices in heterogeneous sites such as forests can be challenging, as they are influenced by other vegetation traits, including canopy and leaf structure, Leaf Area Index (LAI), and Leaf Mass per Area (LMA) (Elsherif et al., 2019; Junttila et al., 2019; Zarco-Tejada et al., 2003). Furthermore, estimating vegetation water status metrics from optical remote sensing data ignores the vertical heterogeneity in canopy biochemical and biophysical traits, caused by the different illumination conditions of leaves along the canopy foliage-height profile, although such heterogeneity determines how light scatters within canopy (Gara et al., 2018; Parker et al., 2001). Recent attempts to overcome this limitation involved the use of multi-wavelength Terrestrial Laser Scanning (TLS) to retrieve canopy water status metrics in three dimensions (Batchelor et al., 2023; Elsherif et al., 2019; Junttila et al., 2019). However, such attempts have been thus far limited to estimating area-based metrics such as EWT.

Another leaf trait that can reflect the vegetation water status is the leaf water mass (g), which is the difference between the leaf fresh and dry weights. It was reported to be a robust predictor of whole-leaf photosynthesis, more so than leaf nitrogen (Wang et

* Corresponding author

al., 2022), and can be used to determine the leaf absolute water content (leaf water mass divided by leaf dry mass, g g^{-1}), which can accurately describe the water deficiency in plants (Ievinsh, 2023). In addition, by measuring leaf water mass at canopy level, the Canopy Water Content (CWC, kg m^{-2}), a key parameter in studying the role of forests in the water cycle, can be estimated. Nevertheless, leaf water mass remains under-investigated, mainly because it is difficult to measure at canopy level, as it requires defoliating the canopy (Baldacci et al., 2017). Recent studies have displayed the potential of terahertz quantum cascade lasers to measure leaf water mass non-destructively (Baldacci et al., 2017; Ievinsh, 2023; Wang et al., 2022). Nonetheless, the applicability of the method in a real forest environment remains unexamined.

In this study, a novel, non-destructive approach was developed and used to estimate leaf water mass at canopy level in three dimensions for six forest canopies in Wytham Woods, Oxford, UK, utilizing the structural and spectral data retrieved from two commercial TLS instruments. The TLS data were used to generate tree 3D models and 3D distributions of leaf area within the canopy. Afterwards, the 3D EWT estimates of the same trees, generated in Elsherif et al. (2019), were coupled with the 3D leaf area distributions to retrieve the distribution of leaf water mass at canopy scale.

2. METHODS

2.1 TLS data and 3D EWT estimates

The dataset used in this study was acquired in a 35×45 m rectangular plot at Wytham Woods (51.78° N, 1.31° W) in Oxfordshire, UK. The site was scanned with the Leica P40 and the Leica P20 TLS instruments (1550 nm and 808 nm, respectively) from multiple scanning positions. Elsherif et al. (2019) describes in detail how 3D EWT distributions were generated and validated at canopy level for 13 trees from four different species: *Quercus robur* (oak), *Acer pseudoplatanus* (sycamore), *Fagus sylvatica* (beech), and *Fraxinus excelsior* (ash). Firstly, the intensity data from the two TLS instruments were calibrated to apparent reflectance then combined on a point-by-point basis in a Normalized Difference Index (NDI) that was linked to EWT using leaf samples. The NDI was then used to estimate EWT at canopy level for the trees of interest, and the estimates were validated using an independent set of leaf samples (274 leaves). The EWT point-clouds were used to separate foliage from wood using a threshold and manual refinements. Six out of the thirteen trees, three oak trees, two sycamore tree, and one beech tree, were chosen to be included in this study.

2.2 Tree 3D models

The 3D EWT point-clouds of the selected six trees, each split into foliage and wood, were imported into CloudCompare v. 2.11.3 software. The cloud normals were computed by assuming that each leaf surface can be approximated as a plane oriented in space, consisting of a set of neighbour points. The search radius for neighbours was selected by the cloud normals computing module to be 30 cm, based on the number of points in the point-cloud and the point spacing. Afterwards, a Poisson surface reconstruction module, which can generate triangle meshes from a point-cloud using the computed cloud normals and the algorithm described in detail in Kazhdan et al., (2013), was applied to each tree point-cloud and 3D leaf and wood models were generated. The octree depth was selected as 10, as the default value of 8 produced distorted meshes, whilst values

more than 10 consumed significantly more processing time without producing noticeable improvements to the quality of the generated mesh.

Next, remaining noise was removed from the 3D models using the density histogram (number of points involved in creating each triangle in the mesh) to filter out the triangles that had very low point density, guided by visual inspection of the meshes and original point clouds. That is, any mesh that occupied an area that was empty in the point cloud was erased. To evaluate the accuracy of the 3D models creation, canopy LAI of each tree was calculated from its 3D model. Although reference canopy LAI values for the exact trees used in this study weren't available, the estimated LAI values were compared to the forest's census data for the same tree species. Following the noise removal step, foliage 3D model of each tree was split into multiple layers (1 m deep), matching the layers of its corresponding 3D EWT point cloud. Furthermore, foliage 3D models were divided into voxels ($0.5 \text{ m} \times 0.5 \text{ m} \times 0.5 \text{ m}$).

2.3 Generating canopy 3D water mass distributions

For each tree 3D model, vertical profiles of leaf area were generated by calculating the total leaf area of each canopy layer and plotting it against the layer's height. In addition, the total leaf area of each layer was multiplied by its EWT to estimate the layer's water mass, then water mass vertical profiles were generated. Similarly, EWT of each voxel in each layer was multiplied by total leaf area in that voxel to estimate the water mass per voxel and generate voxel-based canopy 3D water mass distribution.

Validating the estimated canopy water mass directly using destructing sampling wasn't possible, as it would have required defoliating the whole canopy, or a set of canopy layers, to measure the water mass of each leaf then calculate the total water mass per canopy or layer. Thus, the accuracy of the water mass estimates was evaluated based on the accuracy of canopy EWT and LAI retrieval.

3. RESULTS AND DISCUSSION

Table 1 shows tree height, total leaf area, LAI, and water mass, derived from the generated 3D models, whilst Figure 1 displays the 3D models (not to scale). The results revealed that the oak trees had the highest total canopy leaf area (average of 356 m^2), while the sycamore tree had an average total leaf area of 225.6 m^2 . The lowest leaf area was observed in the beech tree (116.4 m^2). As for the LAI, the oak trees had an average LAI of $5.6 \text{ m}^2 \text{ m}^{-2}$, while average LAI of the sycamores was $5.5 \text{ m}^2 \text{ m}^{-2}$. The beech tree had the lowest LAI ($3.4 \text{ m}^2 \text{ m}^{-2}$). The correlation between canopy total leaf area and canopy LAI was moderate ($R^2 = 0.63$), as canopy LAI was a factor not only of the canopy total leaf area, but also of the canopy projected area.

Tree	Species	Height (m)	Total leaf area (m^2)	LAI ($\text{m}^2 \text{ m}^{-2}$)	Water mass (kg)
1	Sycamore	15.5	181.3	5.4	21.4
2	Sycamore	15	270	5.6	29.1
3	Oak	17.8	361.6	5.5	43.9
4	Oak	16.5	400.5	5.9	54.1
5	Beech	17.5	116.4	3.4	11
6	Oak	16.4	306.7	5.4	38.8

Table 1. Structural parameters and canopy water mass obtained from the 3D models of the six trees.

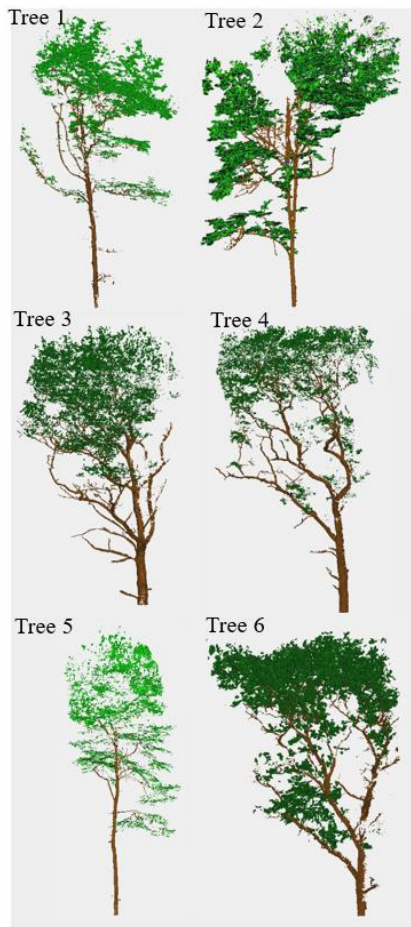


Figure 1. Tree 3D models: trees 1 and 2 are sycamores, trees 3, 4, and 6 are oaks, and tree 5 is beech.

According to the census data available for this region of the forest, average canopy LAI was $5 \text{ m}^2 \text{ m}^{-2}$. This suggested an overestimation of canopy LAI for the sycamore and oak trees by an average of 10% and 12%, respectively. The reason for such overestimation could have been the noise removal stage during the 3D models generation process, as noise filtration was based solely on the visual inspection of each 3D model and its corresponding point cloud. The overestimation of LAI suggested that a percentage of meshes that should have been classified as noise remained in the 3D model. A solution for this issue is selecting a set of trees to serve as calibration data and measuring their canopy LAI in field. The measured LAI values can then be used as constraints in the mesh filtering step to determine a suitable threshold for noise removal using the density histogram.

On the other hand, the beech tree LAI was noticeably underestimated by 32% in comparison to the average LAI measured in the plot. Furthermore, comparing the estimated LAI to beech LAI reported in the literature, which ranged between 4.5 and 5.1, confirmed the underestimation observed in this study. The reason for this was occlusion, as observed in Figure 1, because the beech tree was surrounded by denser oak and sycamore trees in the plot that blocked the laser beams. Occlusion is a known limitation of using TLS to retrieve forest canopy characteristics.

Despite the observed over- and underestimation of canopy LAI, the accuracy obtained using the proposed approach was considered sufficient as it generated tree 3D models from leaf-on TLS data, while the more accurate approaches presented in the literature, such as the use of a Quantitative Structure Model (QSM) to define the structure of canopy woody components, then use leaf insertion algorithms to add the leaves require scanning the forest plot twice in leaf-off and leaf-on conditions.

The estimated canopy water mass revealed that the oak trees contained the highest amount of water with an average of 45.6 kg, followed by the sycamore trees with an average of 25.3 kg, and that the beech tree, for which the estimation was affected by the low LAI, had the lowest water mass (11 kg). Figure 2 displays the relationship between canopy total leaf area and canopy water mass. The figure revealed that the two parameters were highly correlated ($R^2 = 0.98$). This suggested that by measuring canopy LAI using TLS or any other approach, and coupling that with measurements of canopy projected area, the canopy total leaf area can be estimated, which can then be used to retrieve the canopy water mass.

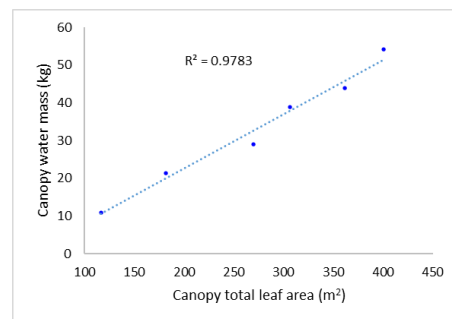


Figure 2. The relationship between canopy total leaf area and canopy water mass.

The vertical profiles of canopy total leaf area and its corresponding water mass, shown in Figure 3, further confirmed that the leaf area per canopy layer was the main factor affecting the water mass in the layer. Furthermore, it was observed that the upper canopy layer in all species had less total leaf area than the mid canopy layers to allow more radiation to enter and scatter within the canopy to improve photosynthesis. The highest water mass was observed in the mid canopy layers. In addition, the figure showed that trees with similar architecture, for instance, tree 3 and tree 4, had similar water mass vertical profiles because of the similarities between their vertical leaf area distributions. However, no similarities were observed between the vertical profiles of canopy EWT and the corresponding water mass vertical profiles.

In all trees, EWT was higher in upper canopy layer than in mid and lower canopy layers, whilst the water mass was higher in mid canopy layers than the remaining layers. The main reason for such observation was that EWT was reported to be highly correlated with LMA, meaning that a thicker leaf would be able to hold more moisture than a thinner leaf (Elshef et al., 2019; Junttila et al., 2019). On the other hand, this study showed that the water mass is dependable on the total leaf area per canopy layer, meaning that the denser a canopy layer is, the more water mass it can hold.

As for the 3D water mass distributions, it was possible to identify individual leaves in tree 3D models and obtain leaf-

level EWT, surface area, and water mass in lower canopy layers, as shown in Figure 4 for a lower canopy layer in tree 2 (sycamore). This has the potential to revolutionize the way tree parameters are retrieved and monitored, as it can provide high resolution estimates while eliminating the need for extensive, time-consuming destructive sampling.

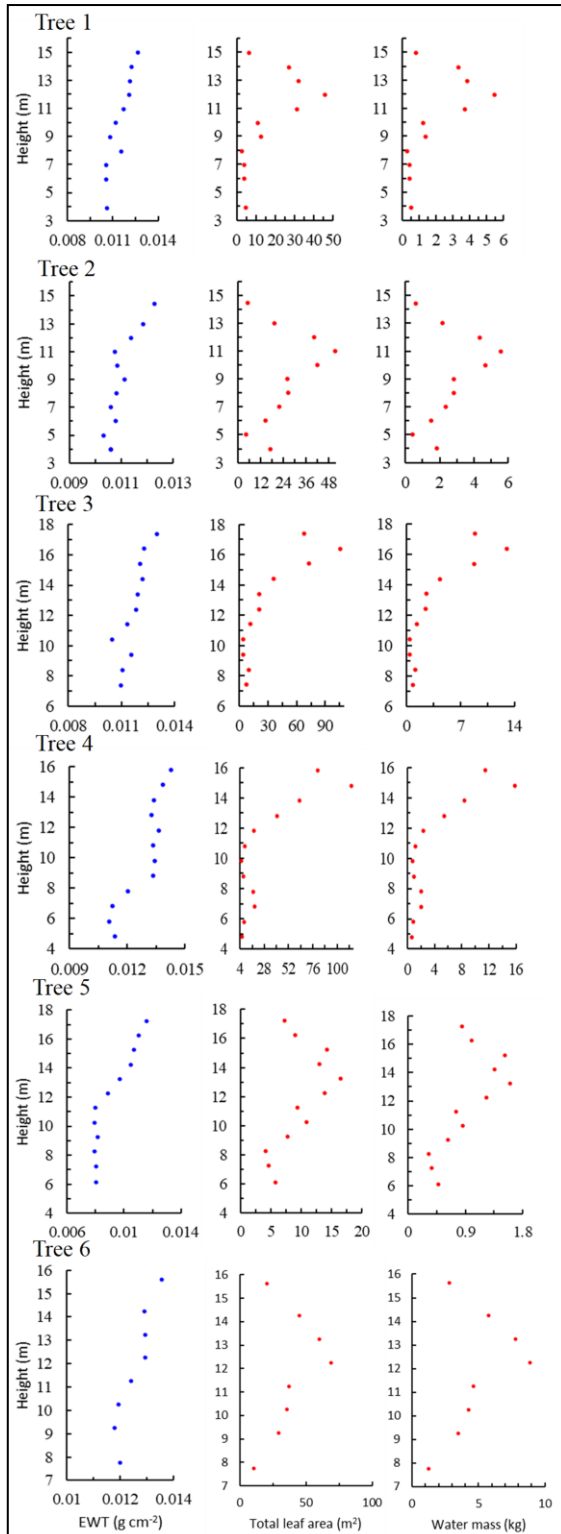


Figure 3. Vertical profiles of canopy EWT, adapted from Elsherif et al., 2019, vertical profiles of total leaf area, and vertical profiles of water mass.

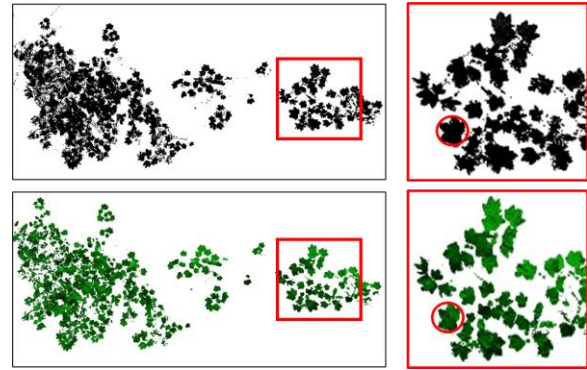


Figure 4. A lower canopy layer in tree 2 (sycamore). Upper is the point cloud and lower is the generated 3D model of the layer. For the highlighted leaf, EWT = 0.009 g cm⁻², surface area = 120.2 cm², and water mass = 1.1 g.

Apart from lower canopy layers, it wasn't possible to identify individual leaves and thus parameters were retrieved per voxel. Figure 5 shows leaf 3D model of tree 6 (oak) and its voxelization (0.5 m × 0.5 m × 0.5 m), where total leaf area, leaf area density, EWT, and water mass are known for each individual voxel. Figure 6 displays the 3D model of the same oak tree and the retrieved voxel-based parameters for a larger voxel (2 m × 2 m × 2 m) for the sake of a clearer visualization.

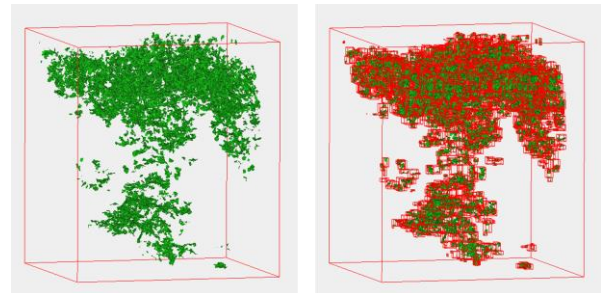


Figure 5. For tree 6 (oak): left is leaf 3D model, whilst right is the voxelized 3D model using 0.5 m × 0.5 m × 0.5 m voxels.

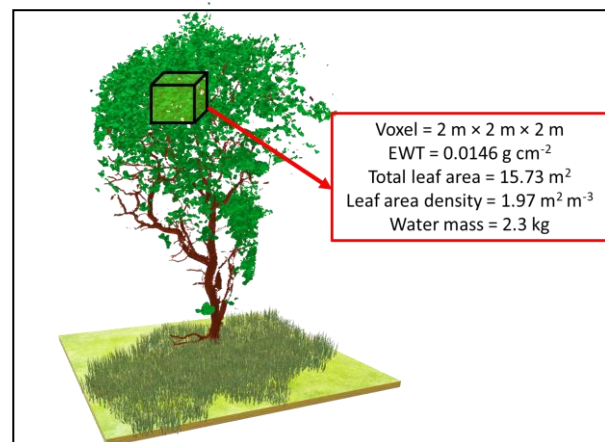


Figure 6. The 3D model of tree 6 (oak) with a single 2 m × 2 m × 2 m highlighted voxel, showing its EWT (g cm⁻²), total leaf area (m²), leaf area density (m² m⁻³), and water mass (kg).

The voxel-based estimates can allow the studying of the distribution of each aforementioned parameter in 3D, examining their horizontal and vertical heterogeneity, and identifying and establishing relationships between them. Furthermore, comparisons between inner and outer canopy parameters can be carried out, as well as linking the 3D water mass distribution to water path length, water potential, illumination conditions, and photosynthesis rate through realistic 3D radiative transfer modelling.

4. CONCLUSIONS

This study introduced a novel approach to generate tree 3D models from dual-wavelength TLS data for six forest canopies from three different species and used the models to estimate the canopy LAI, total leaf area, and vertical profiles of canopy leaf area. Some over- and underestimation was observed in the estimated LAI, indicating that improvements are needed for the proposed approach to enhance the noise removal step during the meshing process. However, the obtained accuracy was considered sufficient as leaf-on point clouds were used to generate the 3D models. In addition, the EWT vertical profiles and canopy leaf area vertical profiles were used to generate vertical profiles of canopy water mass, which showed that the leaf area distribution within the canopy, and the canopy architecture were the main parameters affecting the water mass distribution within the canopy, with mid canopy layers having higher water mass than the other canopy layers. This study showed the potential of TLS to estimate canopy water mass, but controlled experiments that include defoliating canopies are still needed for a direct and accurate validation of the TLS estimates of canopy water mass.

ACKNOWLEDGEMENTS

The data used in this study were collected during a fieldwork campaign, as a part of Ahmed Elsherif PhD study at Newcastle university, UK, which was funded by the Egyptian Ministry of higher education.

REFERENCES

Aerts, R., Honnay, O., 2011: Forest restoration, biodiversity and ecosystem functioning. *BMC ecology*, 11(1), 1-10.

Ali, B., Hafeez, A., Ahmad, S., Javed, M. A., Afridi, M. S., Dawoud, T. M., Almaary, K. S., Muresan, C. C., Marc, R. A., Alkhalifah, D. H. M., Selim, S., 2022. Bacillus thuringiensis PM25 ameliorates oxidative damage of salinity stress in maize via regulating growth, leaf pigments, antioxidant defense system, and stress responsive gene expression. *Frontiers in plant science*, (13) 921668, 1-23.

Baldacci, L., Pagano, M., Masini, L., Toncelli, A., Carelli, G., Storchi, P., Tredicucci, A., 2017. Non-invasive absolute measurement of leaf water content using terahertz quantum cascade lasers. *Plant Methods*, 13, 1-7.

Batchelor, J. L., Rowell, E., Prichard, S., Nemens, D., Cronan, J., Kennedy, M. C., Moskal, L. M., 2023. Quantifying Forest Litter Fuel Moisture Content with Terrestrial Laser Scanning. *Remote Sensing*, 15(6), 1482.

Boyer, J., 1967. Leaf water potentials measured with a pressure chamber. *Plant Physiology*, 42(1), 133-137.

Cochard, H., Forestier, S., Améglio, T., 2001. A new validation of the Scholander pressure chamber technique based on stem diameter variations. *Journal of Experimental Botany*, 52(359), 1361-1365.

Elsherif, A., Gaulton, R., Shenkin, A., Malhi, Y., Mills, J., 2019. Three dimensional mapping of forest canopy equivalent water thickness using dual-wavelength terrestrial laser scanning. *Agricultural and Forest Meteorology*, 276, 107627.

Féret, J. B., Le Maire, G., Jay, S., Berveiller, D., Bendoula, R., Hmimina, G., Cheraïet, A., Oliveira, J. C., Ponzoni, F. J., Solanki, T., De Boissieu, F., 2019. Estimating leaf mass per area and equivalent water thickness based on leaf optical properties: Potential and limitations of physical modeling and machine learning. *Remote Sensing of Environment*, 231, 110959.

Gao, B. C., Goetz, A.F., 1995: Retrieval of equivalent water thickness and information related to biochemical components of vegetation canopies from AVIRIS data. *Remote sensing of environment*, 52(3), 155-162.

Gara, T. W., Darvishzadeh, R., Skidmore, A. K., Wang, T., 2018. Impact of vertical canopy position on leaf spectral properties and traits across multiple species. *Remote sensing*, 10(2), 346.

Ievinsh, G., 2023. Water Content of Plant Tissues: So Simple That Almost Forgotten?. *Plants*, 12(6), 1238.

Junttila, S., Holopainen, M., Vastaranta, M., Lyytikäinen-Saarenmaa, P., Kaartinen, H., Hyypä, J., Hyypä, H., 2019. The potential of dual-wavelength terrestrial lidar in early detection of *Ips typographus* (L.) infestation—Leaf water content as a proxy. *Remote Sensing of Environment*, 231, 111264.

Kazhdan, M., Hoppe, H., 2013: Screened poisson surface reconstruction. *ACM Transactions on Graphics (ToG)*, 32(3), 1-13.

Keenan, R. J., 2015. Climate change impacts and adaptation in forest management: a review. *Annals of forest science*, 72, 145-167.

Kettani, R., Ferrahi, M., Nabloussi, A., Ziri, R., Brhadda, N., 2023. Water stress effect on durum wheat (*Triticum durum* Desf.) advanced lines at flowering stage under controlled conditions. *Journal of Agriculture and Food Research*, (14)100696, 1-12.

Kothari, S., Beauchamp-Rioux, R., Blanchard, F., Crofts, A. L., Girard, A., Guilbeault-Mayers, X., Hacker, P. W., Pardo, J., Schweiger, A. K., Demers-Thibeault, S., Bruneau, A., 2023. Predicting leaf traits across functional groups using reflectance spectroscopy. *New Phytologist*, 238(2), 549-566.

Masson-Delmotte, V., Zhai, P., Pirani, A., Connors, S. L., Péan, C., Berger, S., Caud, N., Chen, Y., Goldfarb, L., Gomis, M. I., Huang, M., 2021. Climate change 2021: the physical science basis. *Contribution of working group I to the sixth assessment report of the intergovernmental panel on climate change*, 2.

Meiyan, S., Qizhou, D., ShuaiPeng, F., Xiaohong, Y., Jinyu, Z., Lei, M., Baoguo, L., Yuntao, M., 2022. Improved estimation of canopy water status in maize using UAV-based digital and

hyperspectral images. *Computers and Electronics in Agriculture*, 197, 106982.

Mengist, W., Soromessa, T., 2019: Assessment of forest ecosystem service research trends and methodological approaches at global level: a meta-analysis. *Environmental Systems Research*, 8(22), 1-18.

Parker, G. G., Lefsky, M. A., Harding, D. J., 2001. Light transmittance in forest canopies determined using airborne laser altimetry and in-canopy quantum measurements. *Remote Sensing of Environment*, 76(3), 298-309.

Rodriguez-Dominguez, C. M., Forner, A., Martorell, S., Choat, B., Lopez, R., Peters, J. M., Pfautsch, S., Mayr, S., Carins-Murphy, M. R., McAdam, S. A., Richardson, F., 2022. Leaf water potential measurements using the pressure chamber: Synthetic testing of assumptions towards best practices for precision and accuracy. *Plant, Cell & Environment*, 45(7), 2037-2061.

Scholander, P. F., Hammel, H. T., Hemmingsen, E. A., Bradstreet, E. D., 1964. Hydrostatic pressure and osmotic potential in leaves of mangroves and some other plants. *Proceedings of the National Academy of Sciences*, 52(1), 119-125.

Seelig, H. D., Hoehn, A., Stodieck, L. S., Klaus, D. M., Adams, W. W., Emery, W. J., 2008. Relations of remote sensing leaf water indices to leaf water thickness in cowpea, bean, and sugarbeet plants. *Remote Sensing of Environment*, 112(2), 445-455.

Sturrock, R. N., Frankel, S. J., Brown, A. V., Hennon, P. E., Kliejunas, J. T., Lewis, K. J., Worrall, J. J., Woods, A. J., 2011. Climate change and forest diseases. *Plant pathology*, 60(1), 133-149.

Tucker, C.J., 1980. Remote sensing of leaf water content in the near infrared. *Remote sensing of Environment*, 10(1), pp.23-32.

Wang, Z., Huang, H., Wang, H., Peñuelas, J., Sardans, J., Niinemets, Ü., Niklas, K. J., Li, Y., Xie, J., Wright, I. J., 2022. Leaf water content contributes to global leaf trait relationships. *Nature Communications*, 13(1), 5525.

Yamasaki, S., Dillenburg, L. R., 1999: Measurements of leaf relative water content in *Araucaria angustifolia*. *Revista Brasileira de fisiologia vegetal*, 11(2), 69-75.

Yilmaz, M. T., Hunt, E. R., Jackson, T. J., 2008. Remote sensing of vegetation water content from equivalent water thickness using satellite imagery. *Remote Sensing of Environment*, 112(5), 2514-2522.

Zarco-Tejada, P. J., Rueda, C. A., Ustin, S. L., 2003. Water content estimation in vegetation with MODIS reflectance data and model inversion methods. *Remote Sensing of Environment*, 85(1), 109-124.

Zhang, Q., Li, Q., Zhang, G., 2012. Rapid determination of leaf water content using VIS/NIR spectroscopy analysis with wavelength selection. *Spectroscopy: An International Journal*, 27(2), 93-105.